



ELSEVIER

Atmospheric Research 70 (2004) 109–130

ATMOSPHERIC
RESEARCH

www.elsevier.com/locate/atmos

Vertical distribution of Saharan dust based on 2.5-year model predictions

P. Alpert, P. Kishcha*, A. Shtivelman, S.O. Krichak, J.H. Joseph

*Department of Geophysics and Planetary Sciences, Faculty of Exact Sciences, Tel Aviv University,
Ramat Aviv, Tel Aviv 69978, Israel*

Received 27 June 2003; accepted 7 November 2003

This study is dedicated to the memory of the seven astronauts of the space shuttle Columbia,
on the mission STS-107

Abstract

Within the framework of the NASA-Israeli MEIDEX project, the averaged 3D-distribution of Saharan dust was estimated and analyzed. This averaged distribution was based on the 2.5-year database of 48-h dust forecasts produced by the dust prediction system, which had been developed earlier at the University of Athens and subsequently modified in Tel Aviv University. The performed climatological analysis is the first one based on a large archive of dust distribution over the whole Sahara and vicinity regions; the total amount of vertical profiles in this archive is approximately 10^7 per year. Vertical distributions of dust reflect differences between the Atlantic and the Mediterranean dust transport. As a whole, the Mediterranean dust is found to be within a wider range of altitudes, penetrating rather higher into the troposphere. On average, dust over the Atlantic penetrates up to ≤ 5 km while over the Mediterranean up to ≤ 8 km. The characteristic feature of dust vertical profiles over the main Saharan dust source near Lake Chad is its maximal concentration near the surface. From April to June averaged profiles over the Chad basin in the Sahara are restricted below the level of ~ 4.5 km. In the winter months and in March, dust concentration over the Chad basin is closer to the surface, under 1.5 km. Dust also maximizes near the surface over another dust source, which is the major one in summer, located in West Africa. These results are consistent with dust-layer altitude ranges from present-day lidar soundings. Besides, the results are in accordance with general synoptic knowledge of the mechanism of dust transport to the Mediterranean. However, only quantitative comparisons of model vertical profiles against lidar measurements, which are under way now, can validate the forecast vertical distribution of Saharan dust.

© 2004 Elsevier B.V. All rights reserved.

Keywords: Dust sources; Dust profiles; Dust prediction; Saharan dust; Atmospheric dust transport; Mediterranean region; Sahara region

* Corresponding author. Fax: +972-3-6409282.

E-mail address: kishcha@hotmail.com (P. Kishcha).

1. Introduction

Information about the vertical distribution of mineral desert dust is required for different climatological applications. Dust absorbs and scatters solar and thermal radiation (Kaufman et al., 2002). Dust-forced cooling/warming of the atmosphere varies as the dust layer ascends or descends. Insufficiency of knowledge about three-dimensional distribution of dust may cause significant errors in the determination of its effect on climate and global warming prediction. Besides, the knowledge of dust vertical distributions is needed for the reliable retrieval of aerosol optical depths from satellite observations (Torres et al., 2002).

Only sparse lidar data about vertical distribution of aerosols are available. These data point to some important features of dust vertical profiles. For example, lidar data from the Lidar In-space Technology Experiment (LITE; <http://asd-www.larc.nasa.gov/ASDhomepage.html>) show dust layers in the boundary layer or above it (Karyampudi et al., 1999). Hamonou et al. (1999) analyzed dust plumes transported to the Mediterranean by two lidar systems in the eastern and western parts of the Mediterranean. According to Hamonou et al. the transported dust over the Mediterranean is concentrated mainly at altitudes between 1.5 and 5 km. The observed dust transport was multilayered; several well-defined layers were detected in the free troposphere. Other lidar observations of Saharan dust, carried out at the island of Lampedusa in the Mediterranean, detected large dust concentrations up to 7 or 8 km in altitude lasting a few days (Di Sarra et al., 2001). During strong perturbations dust can reach up to 10 km in altitude and may last there for several days (Gobbi et al., 2000). At the same time no observation was carried out of the vertical distribution of dust near Lake Chad, which is the most stable source of dust in the Sahara desert as found by Prospero et al. (2002) and Israelevich et al. (2002).

Another approach to indirectly obtaining information about vertical distribution of Saharan dust over the Mediterranean was based on synoptic analysis. The average atmospheric circulation over the Mediterranean does not explain the northward transport of dust particles because winds mostly come from the west or northwest (La Fontaine et al., 1990). Saharan dust is generally transported over the Mediterranean by southerly winds generated by cyclones (Alpert and Ziv, 1989; Moulin et al., 1998). In particular, Alpert and Ziv (1989) found that spring and early summer are the most favorable periods for the development of Sharav cyclones south of the Atlas mountains. Such cyclones move eastward, cross Egypt, Israel and the eastern (and sometimes central) Mediterranean basin. In summer, dust is transported to the western and central parts of the Mediterranean because it is linked with different depression centers (Moulin et al., 1998). Thus, complex wind fields associated with frontal zones drive the transport of dust to the Mediterranean basin. And so, the dust vertical structure may reflect that complexity. This is probably the main reason why the Mediterranean dust transport is different from the Atlantic one (Hamonou et al., 1999).

This study is devoted to a climatological analysis of three-dimensional dust distribution by using the 2.5-year database of dust forecasts. A 3D-dust prediction system was implemented at Tel Aviv University for the 48-h daily prediction of mineral dust over North Africa, the Mediterranean Sea, and a part of the North

Atlantic Ocean since November 2000 (Alpert et al., 2002; Tsidulko et al., 2002). The current analysis was aimed to check the capability of the averaged model outputs to be in line with present-day knowledge on dust distribution within the Sahara desert. In particular, it is important to find out if the model reflects the above mentioned differences between the Atlantic and the Mediterranean dust transport. In addition, it is interesting to get a general view about 3D-dust distribution over North Africa and its month-to-month variations. And finally, the results of dust modelling, accumulated for several years, can be used to create a model of three-dimensional distribution of Saharan dust for several gradations of dust activity. Such a model could be used along with satellite data in order to improve dust vertical initializations for short-term dust and weather predictions.

For these purposes within the NASA-Israeli Mediterranean Dust Experiment (MEIDEX), the database of the 48-h dust forecasts, accumulated at Tel Aviv University over a 2.5-year period, has been adapted for the climatological analysis of dust vertical profiles. The first Israeli astronaut, Ilan Ramon, and his six colleagues of the space shuttle Columbia, who all tragically died on the mission STS-107, participated in the MEIDEX project.

2. Characteristics of the TAU dust prediction system

The dust prediction system, developed earlier at the University of Athens (Nickovic et al., 1997), after modification was put in operative use for short-term dust predictions at Tel Aviv University (Krichak et al., 2002; Alpert et al., 2002; Tsidulko et al., 2002). Results of the daily model predictions are available at the website: <http://earth.nasa.proj.ac.il/dust/current/>. The system is based on the hydrostatic NCEP Eta sigma-eta vertical coordinate model (Mesinger, 1997). The model domain is 0–50°N, 50°W–50°E including the tropical North Atlantic Ocean, North Africa, the Middle East, and the Arabian Peninsula. The model is initialized with the NCEP analysis and the lateral boundary data are updated every 6 h, from the operational forecasts by the NCEP global model. The runs start with 12 UTC and forecasts are performed for 3-h periods up to 48 h.

The model includes packages for dust initialization, transport, and wet/dry deposition, which had been developed at the University of Athens within the framework of the Mediterranean Dust Experiment (MEDUSE) EU project (Nickovic and Dobricic, 1996; Nickovic et al., 1997). All the dust (clay) particles were assumed to be of the effective radius of 2–2.5 μm . This choice fitted the interval of dust particle sizes observed during long-range transport events of North Africa dust (Levin et al., 1980; Perry et al., 1997). Later, Alpert and Ganor (2001) showed that a wide range of dust-particle sizes is typical of those in a heavy dust storm over Israel, and that 2–2.5 μm radius is within the interval of dominant sizes. Today, however, in order to have better estimations of aerosol transport and radiative effects most dust models use at least 2 and as much as up to 10 sizes for dust particles (Kinne et al., in press). For example, the DREAM model (Nickovic et al., 2001), which is based on a modification of the Eta-model,

presented here, uses four different sizes. We understand, on the one hand, that the single-size aerosol is a major shortcoming of the TAU model version, and we are currently experimenting with a number of aerosol sizes. On the other hand, the current model was in operational use without changes during all the period under investigation; hence all model results used in this study are homogeneous. Besides, the choice of the selected size in the current study is justified by satisfactory comparison of the model dust-layer altitude range against lidar observations: an extensive comparison between model dust profiles and Rome lidar soundings is currently being performed (Section 6).

The dust mobilization scheme takes into account the values of the friction and threshold friction velocity, soil wetness and the distribution of the dust source areas, which are specified according to the Olson World Ecosystem data set (Olson et al., 1985). The set contains 59 classes of vegetation with 10' resolution. The mobilized dust particles in the surface layer are driven in a vertical direction by turbulent mixing. The model employs the planetary boundary layer parameterization according to the Monin–Obukhov similarity theory with the use of the Mellor–Yamada Level 2 model. Computation of the relative vertical velocity of the dust particles is executed according to the vertical air velocity and the gravitational settling velocity. The horizontal advection of passive substances (including dust concentration) is performed according to the conservative positive-definite scheme (Janjic, 1990; Nickovic and Dobricic, 1996; Nickovic et al., 1997).

Dust forecasts are initialized with the aid of the Total Ozone Mapping Spectrometer aerosol index (TOMS AI) measurements. This issue was discussed in detail by Alpert et al. (2002). It is well known that one of main problems associated with dust model predictions is the lack of regular dust observations. Before the dust prediction system was put in operational use in November 2000, three possibilities for solving this problem were examined, e.g. zero dust initialization, employing previous dust model output, and employing TOMS AI data. The last option was shown to have an advantage over the others by four skill scores (Alpert et al., 2002, Table 1).

The AI detects aerosols over all land and ocean surfaces, in addition it has the ability to distinguish absorbing aerosols (mineral desert dust, bio-mass burning) from nonabsorbing (sulfate) aerosols (Torres et al., 1998). Indeed, the positive TOMS aerosol indices can not distinguish desert dust from anthropogenic bio-mass burning aerosols. However, in most regions, which we focused on in the current study, in particular in the Mediterranean, dust dominates (Kaufman et al., 2002). The presence of both dust and nonabsorbing air pollution in the same atmospheric volume at the same time will lead to the reduction of the TOMS index.

It is worth noting some disagreement concerning the reliability of the AI calculation below 1 km. Herman et al. (1997) found that UV-absorbing aerosols in the boundary layer near the ground could not readily be detected by the method used for AI calculation. This was because the signal near the ground was weak relative to the apparent noise from the ground. It means that the accuracy of AI is not sufficiently good below 1 km while above 1 km it is better. At the same time, Torres et al. (2002) consider that for mineral dust this restriction for TOMS AI is not so important and AI allows detection of dust particles even close to the ground.

The model initialization with the TOMS aerosol index is performed as follows (Alpert et al., 2002). Initially model-calculated dust profiles, based on a number of model simulations over the Mediterranean and over North Africa, were obtained by employing previous dust model forecasts. The model was initialized with zero dust and was allowed to generate and distribute the dust. The resulting profiles were distributed according to the corresponding TOMS-AI intervals. The initial dust vertical distribution over each grid-point within the model domain was then determined according to the value of TOMS indices among four categories of model-calculated averaged dust profiles over the Mediterranean and among four other profiles over North Africa. Hence, quite different profiles over the Mediterranean and over North Africa were used as explained in Alpert et al. (2002). The four profiles correspond to the average model output profiles at four respective TOMS AI domains of 0.7–1.1, 1.1–1.5, 1.5–1.9 and >1.9.

The dust is considered as a passive substance. No dust feedback effects are included in the radiation transfer calculations.

3. Data and procedure of analysis

This analysis is based on a relatively large archive of vertical profiles over the Sahara; the total number of profiles is approximately 10^7 per year. The database contains a 2.5-year daily data set of 48-h forecasts, obtained for 3-h periods, and is available from November 2000 up to the present. The data are 2D- and 3D-fields of several atmospheric parameters including dust loading, dust concentration, three wind components, temperature, sea level pressure and specific humidity. Horizontal resolution of the model is 0.50 and its vertical resolution—32 eta-levels.

First, the averaged 2D-distribution of dust loading was analyzed to find out if the main structure of simulated dust distribution is associated with the geographical distribution of Saharan dust obtained from previous studies. Then, averaged 3D-distributions were used to get the dust distribution at different altitudes. Several average dust vertical profiles over specific places in the Mediterranean, over Lake Chad basin in the Sahara desert, and in the tropical Atlantic were analyzed comparatively.

We want to focus on the results of atmospheric conditions with dust. The aerosol detection in our approach is based on the TOMS aerosol index. By definition, AI is positive for absorbing aerosols, $-0.2 < AI < 0.2$ in the presence of clouds, and negative for nonabsorbing particles (Torres et al., 2002). The approximation $0.5 AI \cong DL$ between dust loading DL (g/m^2) and AI (Alpert et al., 2002) was used in this study only in order to estimate the dust loading threshold. The threshold $0.1 \text{ g}/\text{m}^2$ was found to correspond to $AI \cong 0.2$ for TOMS. Only vertical dust profiles with dust loading greater than $0.1 \text{ g}/\text{m}^2$ were chosen for the analysis, unless otherwise indicated. It is worth noting that in Alpert et al. (2002) the conversion factor 0.5 in the approximation was only used in order to define the boundaries between the AI categories and relate them to the model-simulated DL. Since these boundaries are to some extent arbitrary, their effects on dust forecast are assumed to be minor.

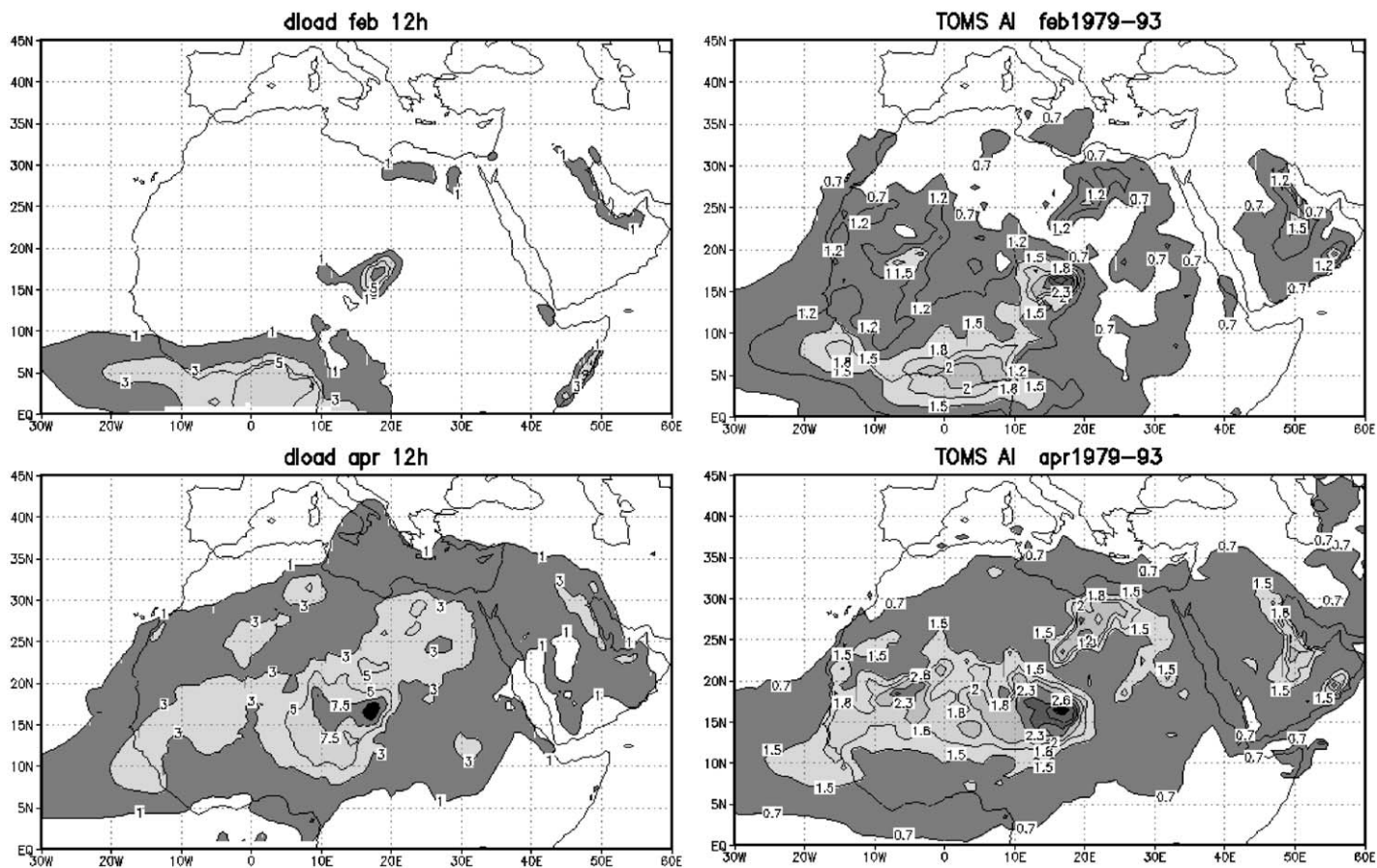


Fig. 1. Comparison between 2D-distributions of model dust loading (10^{-4} kg/m^2), averaged between 2001 and 2002 (left panels), and 2D-distributions of TOMS aerosol index, averaged between 1979 and 1993 (right panels), for February (top row), April (middle row), and June (bottom row).

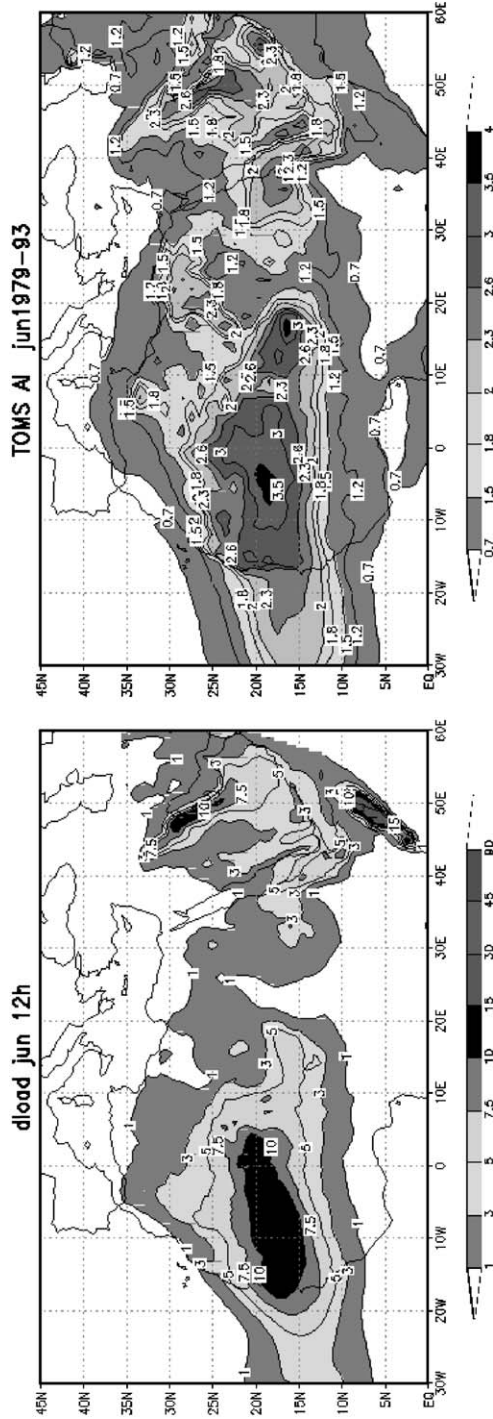


Fig. 1 (continued).

Dust concentration below ~ 700 m was not studied here because of its significant variability, and it will be studied later.

4. Results

4.1. Averaged 2D-distributions of dust loading

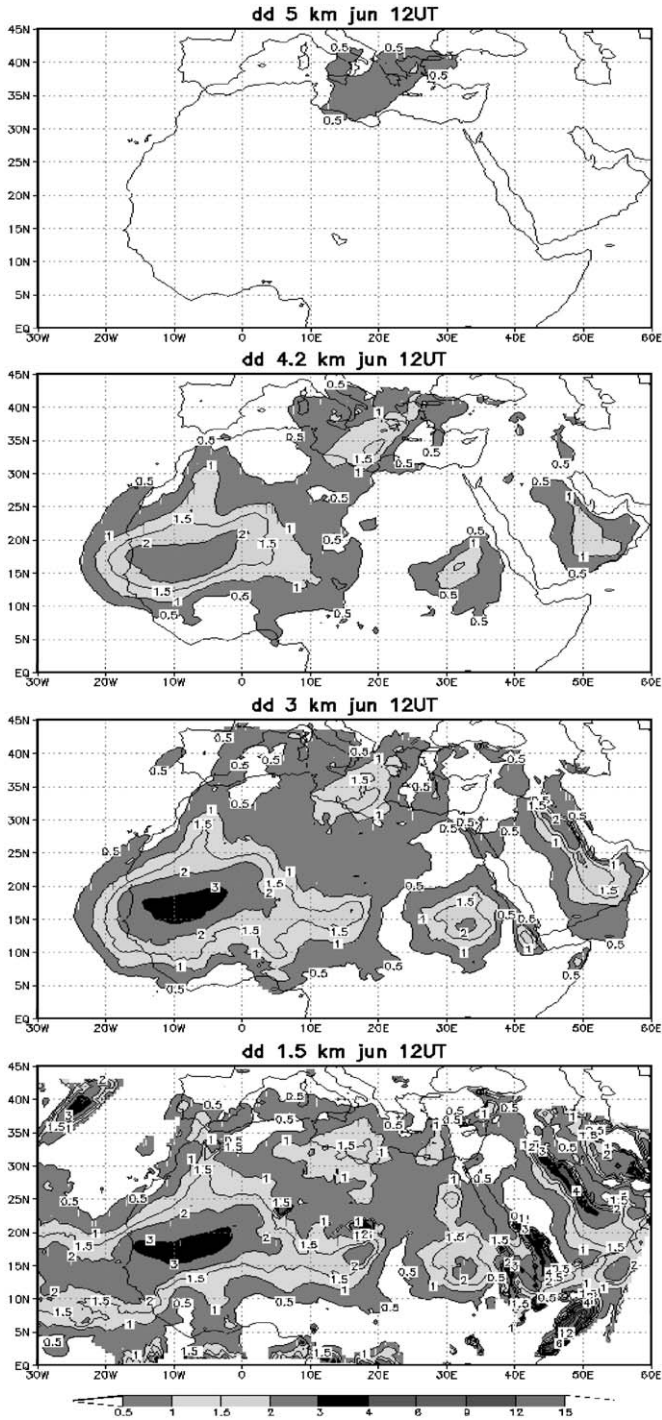
Month-to-month variations of horizontal distribution of dust-loading can be used to evaluate model parameterizations of dust uplift, transport, and deposition as a whole. Since dust loading is defined as the column amount of aerosol in the atmosphere, the local maxima in the 2D-distributions are expected to be located near the largest sources of aerosols. Averaged 2D-distributions of model dust loading show the local maximum over the Lake Chad basin from February to May (Fig. 1). In summer, the area of maximum dust shifts to the western part of Africa. We see that in June the western maximum is the major one. These features are the same as found by Prospero et al. (2002) on the basis of the TOMS aerosol index. Thus, we can conclude that the seasonal cycles of dust activity, as well as the locations of dust maxima, simulated by the model, correspond to Prospero's et al. findings. It should be noted here that in this comparison in Fig. 1 all available model data were used in order to correspond with TOMS monthly averaged data. The 2D-distributions of dust loading, calculated only with the aid of vertical profiles with dust loading greater than 0.1 g/m^2 , are somewhat different from those shown in Fig. 1. On the one hand, they show the same locations of main dust maxima; on the other hand, the noticeable amount of dust over both the Mediterranean Sea and the Atlantic Ocean can be seen. Over the regions where the dust presence is inconstant, these results clearly indicate the necessity of analyzing dust conditions separately from the conditions in dust-free days.

It is worth noting that these 2D-distributions of dust loading do not provide explicitly information on the vertical distribution of dust. However, they indicate that the model as a whole works properly (Section 6).

4.2. Averaged 3D-distributions of dust

This agreement between horizontal distributions of simulated dust loading and observed TOMS aerosol index stimulates interest in a climatological study of 3D-distributions of dust over the extended model domain. Analysis of month-to-month variations of dust concentration at different height levels revealed the following main features of vertical dust distribution. First, dust concentration over the Sahara desert decreases on average as altitude increases. For example, Fig. 2 presents horizontal cross-sections of averaged dust concentration at several height levels: 1.5, 3.0, 4.2 and 5.0 km for the month of June. Besides, Fig. 3 shows similar horizontal distributions for February, April, and June at only two different heights 1.5 and 4.2 km. One can see a peak loading of

Fig. 2. Horizontal distributions of averaged dust concentration (10^{-7} kg/m^3) at different height levels: 1.5, 3, 4.2, and 5 km for the month of June at 12 UTC.



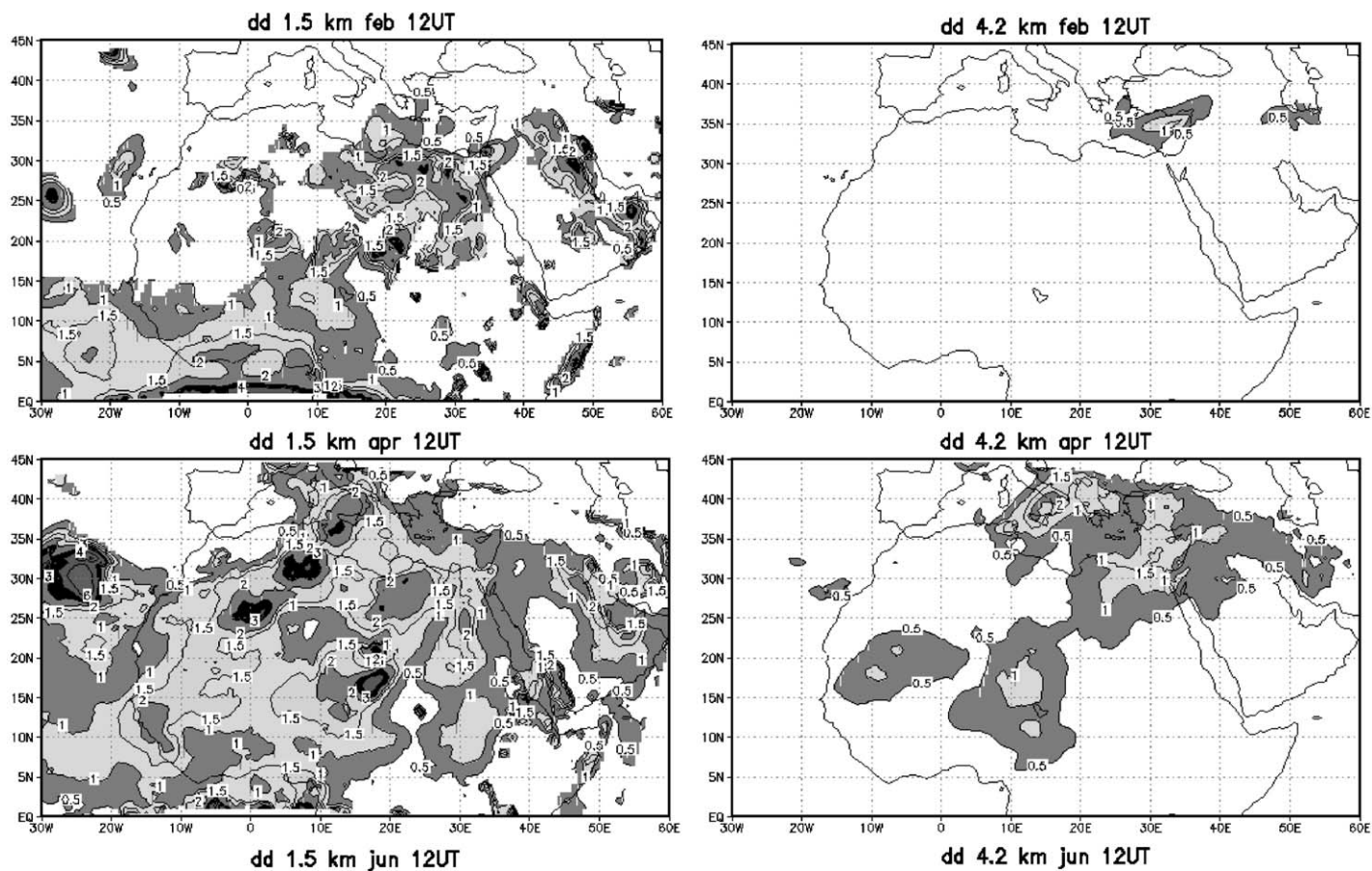


Fig. 3. Horizontal cross-sections of averaged dust concentrations (10^{-7} kg/m^3) at 1.5 km (left panels) and 4.2 km (right panels) over the model domain for February (top row), April (middle row), and June (bottom row).

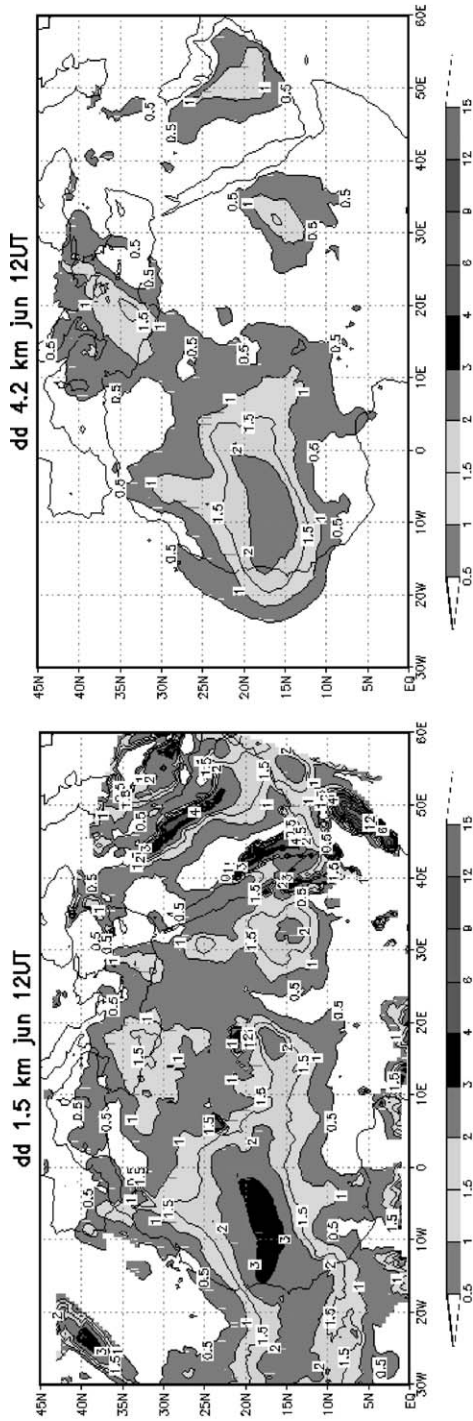


Fig. 3 (continued).

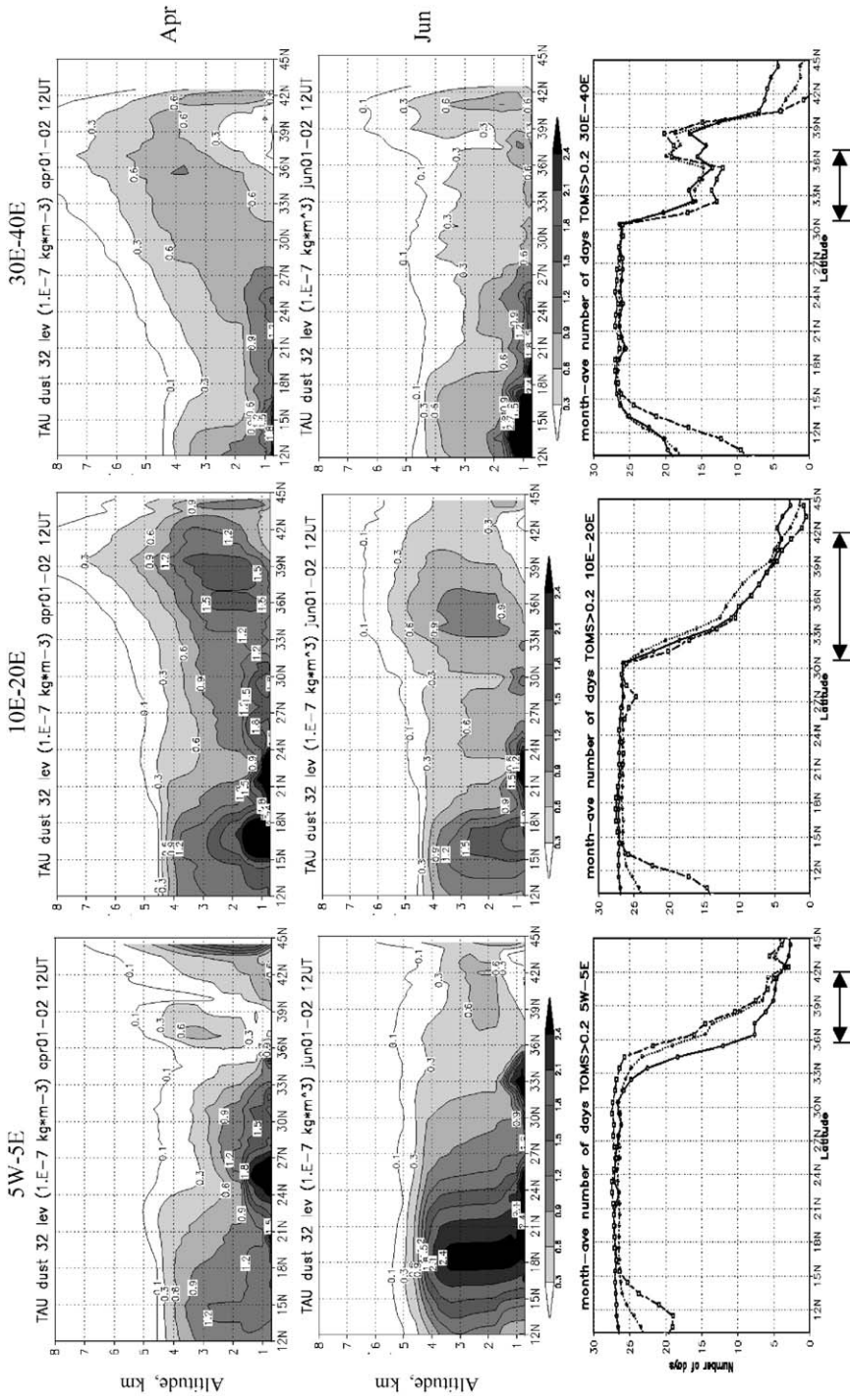
dust at the lowest level 1.5 km for all months. Dust concentration in this layer is maximum over the main dust sources: near Lake Chad and in the Western Sahara. Second, seasonal cycles of dust activity over the Mediterranean differ from that over the tropical Atlantic. Over the tropical Atlantic the extreme dust concentrations are seen in April and June. Over the Mediterranean dust is observed in eastern and central parts in February and April, while in June it shifts to the central and western parts. Finally, dust concentration over the tropical Atlantic decreases with altitude more rapidly than over the Mediterranean. Dust concentration up to 5 km can be seen only over the Mediterranean in Fig. 2.

These results are associated with the present-day conception about the difference between Mediterranean and Atlantic dust intrusions. Since Mediterranean dust intrusions are related to the cyclonic activity around dust sources (Moulin et al., 1998; Alpert and Ziv, 1989), hence dust will be carried by complex wind fields associated with cyclonic frontal conditions. Besides, the high-altitude transport in the Mediterranean can be linked to synoptic uplift, which occurs when the warm Saharan air mass encounters the cooler Mediterranean one. Therefore, in general the Mediterranean dust transport is expected to be within a wide range of altitudes, penetrating rather high into the troposphere and most probably to be multilayered. This conception is supported by lidar data. As mentioned in the Introduction, Hamonou et al. (1999) found multilayered structure of dust in the Mediterranean, concentrated mainly between 1.5 and 5 km. During strong perturbations dust can reach up to a 10-km in altitude and may remain there for several days (Gobbi et al., 2000). The dust within the Saharan Air Layer over the Atlantic is uplifted too, but this is not linked to the cyclonic activity.

In addition to the horizontal cross-sections, it is interesting to analyze vertical cross-sections of average dust concentration. Fig. 4 presents the latitudinal cross-sections for the months of April and June, zonal averaged within three longitudinal zones: 5°W–5°E, 10°E–20°E, and 30°E–40°E. These longitudinal zones were chosen in order to represent vertical distribution of dust over the Western Mediterranean, the Central Mediterranean, and the Eastern Mediterranean respectively. One can see that in the Eastern Mediterranean dust reaches its maximum in spring. In the Central Mediterranean maximum dust concentrations are seen between 1.5 and 4 km of altitude. However, in spring the magnitude of dust concentration in this region is higher than in summer. Moreover, in spring dust in the Central Mediterranean can penetrate higher into the troposphere. Over the Western Mediterranean low dust concentration is seen in April, it is higher in June and reaches its maximum in August (not shown).

In April, maximum dust concentration is seen over the dust source near Lake Chad according to the cross-section zonal average within 10°E–20°E (Fig. 4). As mentioned above, in summer the main maximum of dust shifts to the Western Sahara. One can see in the cross-section zonal averaged within 5°W–5°E that indeed this summer maximum is stronger than the one near Lake Chad. For both these maxima, dust concentration

Fig. 4. Latitudinal cross-sections of dust concentration for the months of April (top panel) and June (middle panel) at 12UTC, zonal averaged within three longitudinal zones: 5°W–5°E, 10°E–20°E, and 30°E–40°E. The bottom panel presents latitudinal variations of the numbers of monthly averaged dusty days when TOMS AI>0.2, averaged within the same longitudinal zones, for the months of April (solid lines), June (dotted lines), and August (dashed lines). The arrows show the latitudinal interval of the Mediterranean Sea.



maximizes near the surface. This is corroborated both by the LITE measurements over the West Coast of Africa and by the GOCART model simulations (Ginoux et al., 2001; Karyampudi et al., 1999).

In our study, dust vertical distribution is analyzed over both North Africa and the Mediterranean including the regions where the dust presence is inconstant. Hence, it is important to estimate the number of dusty days there. The TOMS data for 15 years from 1979 to 1993 were used to produce these estimations. Shown in Fig. 4, bottom panel, are the latitudinal variations (averaged within the aforementioned longitudinal zones) of the number of monthly averaged dusty days, when TOMS AI>0.2. One can see that over North Africa the monthly averaged number of dusty days is about 27 in April, in June, and in August for all three cross-sections. Over the Mediterranean this number decreases with latitude. On average, the number of dusty days in the Western Mediterranean is lower than in other parts of the Mediterranean. In the Eastern Mediterranean the lowest numbers of dusty days are seen in June while in the Central Mediterranean and in the Western Mediterranean the lowest numbers are seen in April.

4.3. Average vertical profiles of Saharan dust

The earlier conclusions concerning the difference between the dust transport over the Mediterranean and the Atlantic is supported by averaged vertical profiles of dust over four small domains (2° latitude by 2° longitude) shown in Fig. 5. Three profiles for the month of June are shown for each domain. One is the average profile, calculated for all available profiles with dust loading greater than 0.1 g/m^2 . The average profile for high (low) dust activity was calculated for only vertical profiles with dust loading greater (less) than normal value.

The distinctive features of profiles over the Mediterranean domains: Sde-Boker and Lampedusa, are clearly seen, in particular, when dust activity is high. The profiles correspond to thick dust layers up to $\leq 8 \text{ km}$ high. In June, dust concentration over Sde-Boker (the Eastern Mediterranean) is not as high as over the island of Lampedusa in the Central Mediterranean. As shown in the previous section, in the Eastern Mediterranean dust reaches its maximum in spring.

These results are consistent with the findings by Alpert and Ziv (1989), Alpert et al. (1990) and Moulin et al. (1998) about major synoptic situations generating the Mediterranean dust transport during spring and summer. As mentioned above the Eastern Mediterranean is exposed to dust mainly in spring and early summer due to Sharav cyclones (Alpert and Ziv, 1989). Alpert et al. (1990) found that the synoptic situation in summer is different. In spite of the fact that Saharan depressions near Atlas still develop, they can not follow a northeastern direction. According to Moulin et al. (1998), the main reason is the presence of a high over Libya. This meteorological situation induces south and southwest winds resulting in dust transport to the Central and Western Mediterranean. Toward the end of summer, Balearic Islands become an active depression center generating dust transport across the Mediterranean in the direction of Corsica and Italy.

The characteristic feature of dust vertical profiles over the dust source near Lake Chad is maximum concentration near the surface (Fig. 5). From April to June averaged profiles

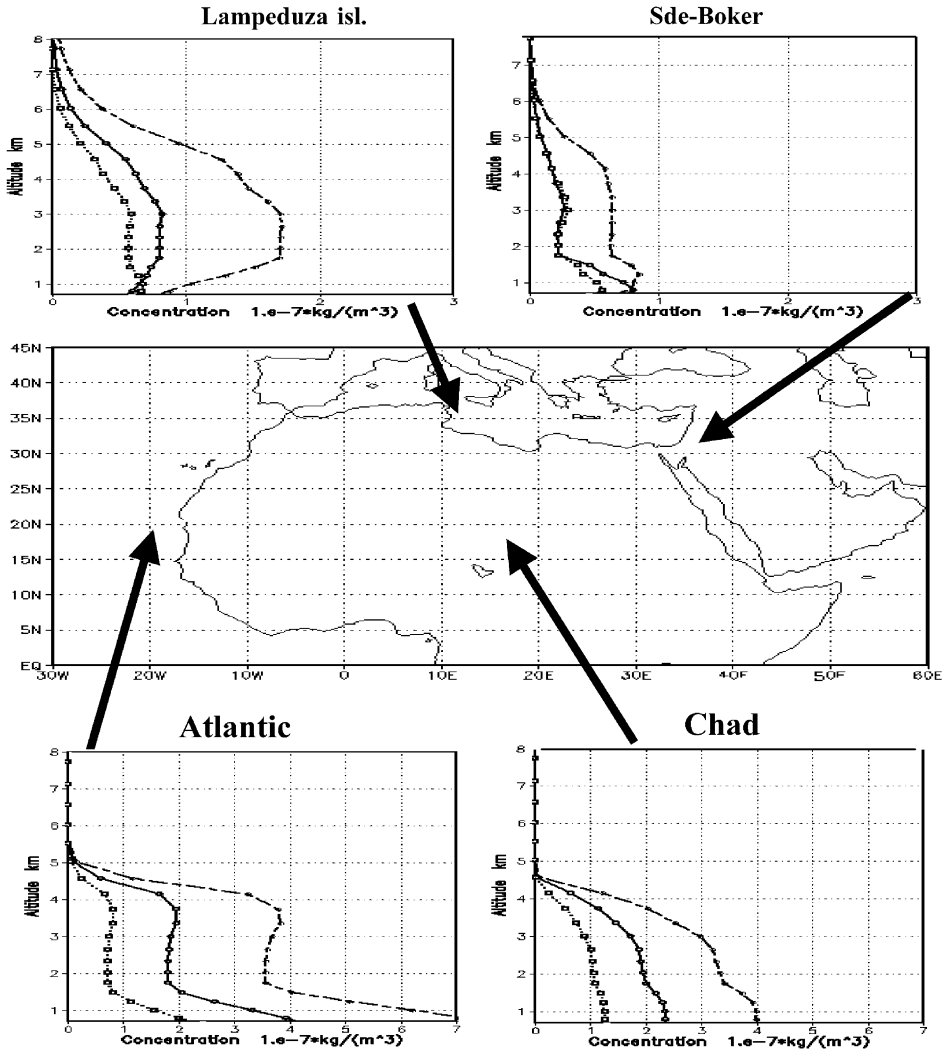


Fig. 5. Average vertical profiles of dust for the month of June at 12UTC over Sde-Boker (Israel) in the Eastern Mediterranean (29.5°N–31.5°N, 34°E–36°E), the Lampedusa island in the Central Mediterranean (34.5°N–36.5°N, 11.5°E–13.5°E), the Chad basin in the Sahara desert (15°N–17°N, 15°E–17°E), and a domain within the Eastern Atlantic (17°N–19°N, 17°W–19°W). The average profiles, calculated for all available profiles for specific month with dust loading greater than 0.1 g/m², are designated by solid line. The average profiles for high (low) dust activity, calculated for only vertical profiles with dust loading greater (less) than normal, are designated

over the Chad basin in the Sahara are restricted to the level ~ 4.5 km altitude. In the winter months and in March, dust concentration over the Chad basin is closer to the surface, below 1.5 km (not shown).

Over the Atlantic, dust penetrates approximately up to ≤ 5 km in altitude. In June dust reaches its maximum there while in winter dust concentration is low. The local extremum between 3 and 4 km in June is clearly seen. Another maximum near the sea surface should be ignored, since it is related to incorrect dust initialization profiles near the sea surface. The possible reasons for dust restraint near the surface in this region are discussed later in Section 6 (Discussion).

4.4. The 48-h and 24-h predictions of dust

This study is based on analysis of 24-h forecasts of dust. It is interesting to find out if there is any error tendency in the 48-h model predictions of dust concentration in relation to 24-h predictions. In order to answer this question, vertical profiles of differences between dust concentration obtained by 48-h and 24-h predictions were analyzed. It was found that these differences could sometimes be significant. However, they are distributed in such a way that their averaged profile gives concentrations close to 0, meaning that there is no pronounced tendency to errors in the 48-h model

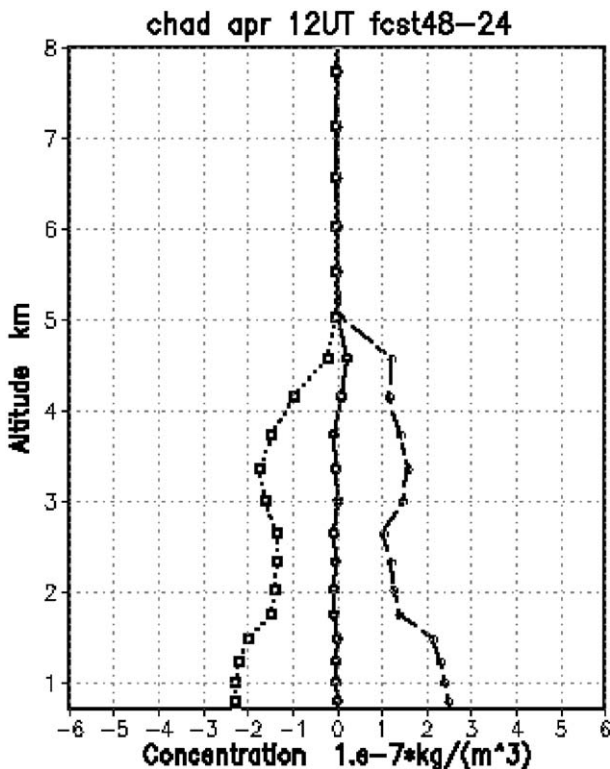


Fig. 6. The average vertical profile of differences between dust concentrations obtained by 48-h and 24-h model predictions (solid line) over the Chad basin. Dashed and dotted lines show vertical profiles of standard deviation, obtained separately for positive and negative differences, respectively.

predictions (Fig. 6). Similar values of standard deviation, obtained for positive and negative differences separately, support this result.

5. Support of dust studies based on reanalysis increments

The average 3D-distribution of Saharan dust can be used in support of dust studies based on the indirect measures of aerosol processes like reanalysis increments (Alpert et al., 1998, 2000; Kishcha et al., 2003). The reanalysis increments are the systematic errors of global climate models, generated in reanalysis procedure. In the recent study by Kishcha et al. (2003) 15 years (1979–93) of the European reanalysis increments (ERA15) from ECMWF were employed in order to analyze dust radiative effects over the Sahara desert. The dust effect was examined by considering the time correlation between the temperature increments and the TOMS aerosol index. The distinctive structure was identified in the distribution of correlation composed of three nested areas with high positive correlation (>0.5), low correlation, and high negative correlation (<-0.5). The innermost positive correlation area (PCA) was a large area ($15^{\circ}\text{N}-30^{\circ}\text{N}$, $5^{\circ}\text{E}-20^{\circ}\text{E}$) near the center of the Sahara desert. For some local maxima inside this area the correlation even exceeded 0.8. Our derived vertical profiles of correlation inside this area show positive high correlation at pressure levels

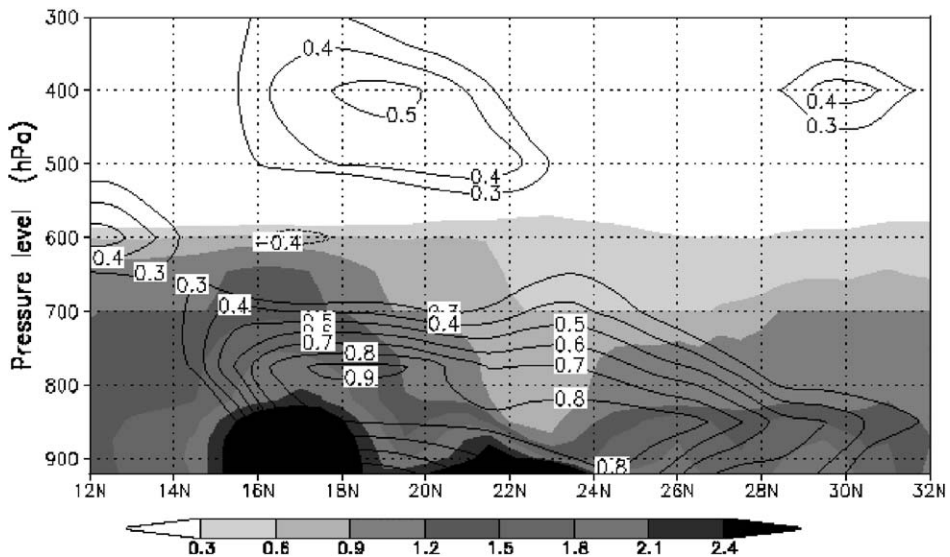


Fig. 7. Vertical distribution of averaged model dust concentration and the one of correlation within the latitudinal cross-section zonal averaged over PCA both in the daytime (12 UTC) in the month of April. Solid lines show the correlation between the ECMWF temperature increments at the ERA model levels and the TOMS aerosol index during the period from 1979 to 1993. The model dust concentration (10^{-7} kg/m^3) averaged for the month of April 2001–2002 is shown by grayscale shades.

ranging from 850 to 700 h Pa. The positive (negative) correlation suggests that the atmosphere becomes warmer (cooler) with dust.

This analysis of the spatial distribution of the time correlation can expand our knowledge of dust radiative effects if we come up with a correct interpretation of the results. Comparing the spatial distribution of correlation with the one of dust itself can help here. In circumstances when there are no observations of dust vertical distributions near Lake Chad, we can use the average 3D-distribution based on dust model predictions. Shown in Fig. 7, is the comparison between the vertical distribution of average model dust concentration and the one of correlation within the latitudinal cross-section zonal averaged over PCA both in the daytime (12 UTC) in the month of April. One can see that the extreme zone of high positive correlation is located in the upper part of the dust layer. This result, relevant for the thick dust layers in PCA, is associated primarily with the direct solar heating of the dust layer due to absorption of short wave (solar) radiation (Kishcha et al., 2003). In other words, the result suggests that the upper part of such a dust layer is heated mainly by the absorption of solar radiation from above rather than by the upward air flow from the surface.

6. Discussion

We found that the average 3D-distribution of Saharan dust correctly reflects differences between the tropical Atlantic and the Mediterranean dust transport. Specifically, the Mediterranean dust layer is located within a wider range of altitudes, penetrating higher into the troposphere.

Our results are in agreement with the outcomes of synoptic analyses by Alpert and Ziv (1989), Moulin et al. (1998) and Tsidulko et al. (2002). They found a relationship between Mediterranean dust intrusions and cyclonic activity around dust sources in North Africa. Cyclonic frontal conditions as well as synoptic uplift of warm Saharan air over the cooler Mediterranean one, are the causal factors of dust penetration high into the troposphere. These findings are supported by available lidar data (Gobbi et al., 2000; Di Sarra et al., 2001; Hamonou et al., 1999). Thus, three independent approaches: (1) our model data, (2) synoptic analysis, and (3) lidar measurements, lead to similar conclusions.

One point, which needs clarification, is the dust vertical distribution over the Atlantic. According to the Saharan dust plume conceptual model by Karyampudi and Carlson (1988), Karyampudi et al. (1999), over the latitudinal belt of 10°N–30°N dust is carried from the Sahara within a mixed layer called the Saharan Air Layer (SAL). The height of the SAL typically extends to 500 mb (6 km). Its base is near the surface over the West Sahara. But it rises quite rapidly in a westward direction, reaching about 850 mb (~ 1.5 km) at longitude ~ 25°W. The Karyampudi et al. model was validated by the lidar measurements on board the space shuttle from the LITE experiment over the eastern Atlantic region. These lidar measurements showed the top of the dust layer at 4.5–5.5 km, which is consistent with our model vertical profiles over the Atlantic. Near the base of the SAL, the dry and hot air mass forms a temperature inversion. This inversion in the case of incorrect dust initialization profiles near the sea surface in this region, could be a causal factor which did not let our model redistribute dust concentration properly.

This fact may be considered as another significant difference between the dust vertical distribution over the Atlantic Ocean and the Mediterranean Sea. Intensive convection processes over the Mediterranean could apparently destroy the low-level inversion and redistribute dust concentration in the correct way unlike the processes over the Atlantic (Tsidulko et al., 2002).

Section 5 shows how to come up with a solution in the most common circumstances when dust vertical distributions are not available, like near Lake Chad, for example. We can estimate the averaged 3D-distribution based on dust model predictions. Of course, possible incorrect estimates of the aerosol vertical distribution may add a bias to the interpretation of results of the temperature increment analysis described in Section 5. A comparison of the model results against lidar observations would be very helpful to better understand the model capabilities. In this connection it is worth noting the existence of some problems with using of available lidar data. As is well known, lidars represent the most efficient technique for the observation of vertical distribution of atmospheric aerosols. As shown above, the lidar data were successfully used in this study to estimate the range of altitudes where dust is located in the atmosphere. However, the quantitative comparison between lidar signals and the model vertical distribution of dust is problematic. As a matter of fact, a comprehensive model of functional relationships, linking aerosol backscatter with aerosol extinction and volume, is needed. Recently such a model for the desert-dust case was developed by Barnaba and Gobbi (2001). It is worth noting that the model errors associated with resulting profiles of aerosol volume are of the order of 100%. Despite this, joint activities with Barnaba and Gobbi comparing our dust-predicted profiles with their lidar observations are in progress now. For instance, the profiles, which showed high dust volume up to approximately 6 km during a very strong dust intrusion over Rome on 12 April 2002, were predicted by our model, and corroborated by lidar data.

It seems reasonable to assume that dust always maximizes at the surface near dust sources. The obtained averaged vertical profiles over the Chad basin fit this assumption. There are no available observations in this region in order to corroborate this result. On the other hand, near another source in the Western Sahara aerosol backscattering measurements during the LITE experiment showed similar specific features of dust. This was also supported by the vertical distributions of dust simulated by the GOCART model (Ginoux et al., 2001).

Month-to-month variations of the horizontal distribution of simulated dust loading are associated with seasonal cycles of dust activity as reflected in the TOMS aerosol index. The distributions of the largest sources of dust in the Sahara, simulated by the model, are in agreement with the TOMS measurements. As mentioned in Section 1, this study should validate the forecast height profiles. It may be argued that this aim can not be reached by comparing model 2D-distributions with those based on the TOMS data. The following two arguments may be presented in this context: First, 2D-distributions show nothing on the vertical distribution. Second, the model 2D-distributions should be comparable with the TOMS measurements since the model is initialized with the TOMS data. However, the distinctive feature of our approach, which is based on the data set of model-predicted vertical profiles, is noteworthy. In Fig. 1 the 2D-distributions of dust loading for 24-h forecasts are analyzed. For 24 h the model can significantly change dust concentrations

in the atmosphere. In order to check if 24 h was enough to validate the model, we compared 48-h and 24-h forecasts in Section 4.4. It was found that on average the vertical profiles of the differences between dust concentrations, obtained by 48-h and 24-h predictions, are negligible. Dust loading in the model is calculated with the aid of vertical profiles. It means that there is a functional relationship between them. Hence, the agreement between the simulated dust loading for 24-h forecasts and the TOMS measurements, is a good indicator that the model as a whole works properly and produces consistent vertically integrated results.

7. Conclusions

The performed analysis is the first one based on a relatively large archive of dust distribution over the whole Sahara and vicinity regions. The used 2.5-year database of 48-h dust forecasts was produced by the dust prediction system, which had been developed earlier at the University of Athens and subsequently modified at Tel Aviv University. Our 2.5-year experience of using the TAU dust prediction model tells us that its performance is good and this makes it appropriate for regular regional dust forecasting. The model was also successfully employed in the MEIDEX experiment with the space shuttle Columbia participation.

Vertical distributions of dust reflect differences between the Atlantic and the Mediterranean dust transport. As a whole, the Mediterranean dust is found to be within a wider range of altitudes, penetrating rather higher into the troposphere. The characteristic feature of dust vertical profiles over the dust source near Lake Chad is its maximal concentration near the surface. Dust also maximizes near the surface over another dust source, which is the major one in summer, located in West Africa. These results are consistent with dust-layer altitude ranges from present-day lidar soundings.

Month-to-month variations of horizontal distribution of simulated dust loading correspond with known seasonal cycles of dust activity based on the TOMS aerosol index. The distributions of the largest sources of dust in the Sahara, simulated by the model, are in agreement with the TOMS measurements. However, only quantitative comparisons of model vertical profiles against lidar measurements, which are under way now, can validate the forecast vertical distribution of Saharan dust.

Acknowledgements

This research was supported by Israeli Space Agency (ISA) as part of the Mediterranean Israeli Dust Experiment (MEIDEX). The latter is a joint project between ISA and NASA. The study was also supported by the EU DETECT Project (Contract No.: EVK2-CT-1999-00048), and the grant GLOWA-Jordan River from the Israeli Ministry of Science and Technology together with the German Bundesministerium fuer Bildung and Forschung (BMBF). The authors wish to acknowledge B. Starobinez for the encouragement and help. The remarks of two anonymous referees improved the clarity of the paper, and we are grateful to them.

References

- Alpert, P., Ziv, B., 1989. The Sharav cyclone: observations and some theoretical considerations. *J. Geophys. Res.* 94, 18495–18514.
- Alpert, P., Neeman, B.U., Shay-El, Y., 1990. Climatological analysis of Mediterranean cyclones using ECMWF data. *Tellus* 42A, 65–77.
- Alpert, P., Kaufman, Y.J., Shay-El, Y., Tanre, D., da Silva, A., Schubert, S., Joseph, J.H., 1998. Quantification of dust-forced heating of the lower troposphere. *Nature* 395, 367–370.
- Alpert, P., Herman, J., Kaufman, Y.J., Carmona, I., 2000. Response of the climatic temperature to dust forcing, inferred from total ozone mapping spectrometer (TOMS) aerosol index and the NASA assimilation model. *Atmos. Res.* 53, 3–14.
- Alpert, P., Ganor, E., 2001. Saharan mineral dust measurements from TOMS: Comparison to surface observations over the Middle East for the extreme dust storm, March 14–17, 1998. *J. Geophys. Res.* 106, 18,275–18,286.
- Alpert, P., Krichak, S.O., Tsidulko, M., Shafir, H., Joseph, J.H., 2002. A dust prediction system with TOMS initialization. *Mon. Weather Rev.* 130 (9), 2335–2345.
- Barnaba, F., Gobbi, G.P., 2001. Lidar estimation of tropospheric aerosol extinction, surface area and volume: maritime and desert-dust cases. *J. Geophys. Res.* 106 (D3), 3005–3018.
- Di Sarra, A., Di Iorio, T., Cacciani, M., Fiocco, G., Fua, D., 2001. Saharan dust profiles measured by lidar at Lampedusa. *J. Geophys. Res.* 106, 10335–10347.
- Ginoux, P., Chin, M., Tegen, I., Prospero, J.M., Holben, B., Dubovik, O., Lin, S.-J., 2001. Sources and distributions of dust aerosols simulated with the GOCART model. *J. Geophys. Res.* 106, 20255–20274.
- Gobbi, G.P., Barnaba, F., Giorgi, R., Santacasa, A., 2000. Altitude-resolved properties of a Saharan dust event over the Mediterranean. *Atmos. Environ.* 34, 5119–5127.
- Hamonou, E., Chazette, P., Balis, D., Dulac, F., Scheider, X., Galani, E., Ancellet, G., Papayannos, A., 1999. Characterization of the vertical structure of Saharan dust export to the Mediterranean basin. *J. Geophys. Res.* 104, 22257–22270.
- Herman, J.R., Bhartia, P.K., Torres, O., Hsu, C., Sefstor, C., Celarier, E., 1997. Global distribution of UV-absorbing aerosol from Nimbus-7/TOMS data. *J. Geophys. Res.* 102, 16911–16922.
- Israelevich, P.L., Levin, Z., Joseph, J.H., Ganor, E., 2002. Desert aerosol transport in the Mediterranean region as inferred from the TOMS aerosol index. *J. Geophys. Res.* 107 (D21), 4572 (10.1029/2001JD002011).
- Janjic, Z.I., 1990. The step-mountain coordinate: physical package. *Mon. Weather Rev.* 118, 1429–1443.
- Karyampudi, V.M., Carlson, T.N., 1988. Analysis and numerical simulations of the Saharan air layer and its effect on easterly wave disturbances. *J. Atmos. Sci.* 45, 3102–3136.
- Karyampudi, V.M., Palm, S.P., Reagan, J.A., Hui, F., Grant, W.B., Hoff, R.M., Mouline, H.R., Pierce, H.F., Torres, O., Browell, E.D., Melfi, S.H., 1999. Validation of the Saharan dust plume conceptual model using lidar, Meteosat, and ECMWF data. *Bull. Am. Meteorol. Soc.* 80 (6), 1045–1075.
- Kaufman, Y.J., Tanre, D., Boucher, O., 2002. A satellite view of aerosols in the climate system. *Nature* 419, 215–223.
- Kinne, S., Lohmann, U., Ghan, S., Easter, R., Chin, M., Ginoux, P., Takemura, T., Tegen, I., Koch, D., Herzog, M., Penner, J., Pitari, G., Holben, B., Eck, T., Smirnov, A., Dubovik, O., Slutsker, I., Tanre, D., Torres, O., Mishchenko, M., Geogdzhayev, I., 2003. Monthly averages of aerosol properties: a global comparison among models, satellite data and AERONET ground data. *J. Geophys. Res.* (in press).
- Kishcha, P., Alpert, P., Barkan, J., Kirchner, I., Machenhauer, B., 2003. Atmospheric response to Saharan dust deduced from ECMWF reanalysis increments. *Tellus* 55B (4), 901–913.
- Krichak, S.O., Tsidulko, M., Alpert, P., 2002. A study of an INDOEX period with aerosol transport to the Eastern Mediterranean area. *J. Geophys. Res.* 107 (D21), 4582 (doi: 10.1029/2001JD001169).
- La Fontaine, C.V., Bryson, R.A., Wendland, W.M., 1990. Airstream regions of North Africa and the Mediterranean. *J. Clim.* 3, 366–372.
- Levin, Z., Joseph, J.H., Mekler, Y., 1980. Properties of Sharav (Khamsin) dust-comparison of optical and direct sampling data. *J. Atmos. Sci.* 37, 882–891.
- Mesinger, E., 1997. Dynamics of limited area models: formulation and numerical methods. *Meteorol. Atmos. Phys.* 63, 3–14.

- Moulin, C., Lambert, C., Dayan, U., Masson, V., Ramonet, M., Bousquet, P., Legrand, M., Balkanski, Y., Guelle, W., Marticorena, B., Bergametti, G., Dulac, F., 1998. Satellite climatology of African dust transport in the Mediterranean atmosphere. *J. Geophys. Res.* 103, 13137–13144.
- Nickovic, S., Dobricic, S., 1996. A model for long-range transport of desert dust. *Mon. Weather Rev.* 124, 2537–2544.
- Nickovic, S., Kallos, G., Kakaliagou, O., Jovic, D., 1997. Aerosol production/transport/deposition processes in the Eta model: desert cycle simulations. Preprints. Proc. Symp. on Regional Weather Prediction on Parallel Computer Environments, University of Athens, Athens, Greece, pp. 137–145.
- Nickovic, S., Kallos, G., Papadopoulos, A., Kakaliagou, O., 2001. Model for prediction of desert dust cycle in the atmosphere. *J. Geophys. Res.* 106, 18113–18130.
- Olson, J.S., Watts, J.A., Alison, L.J., 1985. Major world ecosystem complexes ranked by carbon in live vegetation. Carbon Dioxide Information Center Report NDP-017. Oak Ridge National Laboratory, Oak Ridge, TN, 288 pp.
- Perry, K.D., Cahill, T.A., Eldred, R.A., Dutcher, D.D., 1997. Long-range transport of North African dust to the eastern United States. *J. Geophys. Res.* 102, 11225–11238.
- Prospero, J.M., Ginoux, P., Torres, O., Nicholson, S., Gill, E., 2002. Environmental characterization of global sources of atmospheric soil dust identified with the NIMBUS-7 total ozone mapping spectrometer (TOMS) absorbing aerosol product. *Rev. Geophys.* 40 (1), 1002 (doi:10.1029/2000RG000095).
- Torres, O., Bhartia, P.K., Herman, J.R., Ahmad, Z., Gleason, J., 1998. Derivation of aerosol properties from satellite measurements of backscattered ultraviolet radiation: theoretical basis. *J. Geophys. Res.* 103 (D14), 17099–17110.
- Torres, O., Bhartia, P.K., Herman, J.R., Sinyuk, A., Ginoux, P., Holben, B., 2002. A long-term record of aerosol optical depth from TOMS observations and comparison to AERONET measurements. *J. Atmos. Sci.* 59, 398–413.
- Tsidulko, M., Krichak, S.O., Alpert, P., Kakaliagou, O., Kallos, G., Papadopoulos, A., 2002. Numerical study of a very intensive eastern Mediterranean dust storm, 13–16 March 1998. *J. Geophys. Res.* 107 (D21), 4581 (doi: 10.1029/2001JD001168).